remote sensing

Detecting the Effects of Extreme Events on Estuarine Suspended Particulate Matter Using Satellite Remote Sensing (Scheldt Estuary): Challenges and Opportunities

Juliana Tavora [1,*], Mhd. Suhyb Salama [1], Marloes Penning de Vries [1], Chris M. Mannaerts [1], and Daphne van der Wal [1,2]

[1] Faculty of Geo-Information Science and Earth Observation (ITC), University of Twente, P.O. Box 217, 7500 AE Enschede, The Netherlands; s.salama@utwente.nl (M.S.S.); m.j.m.penningdevries@utwente.nl (M.P.d.V.); c.m.m.mannaerts@utwente.nl (C.M.M.); d.vanderwal@utwente.nl (D.v.d.W.)

[2] NIOZ Royal Netherlands Institute for Sea Research, Dept of Estuarine and Delta Systems, P.O. 140, 4400 AC Yerseke, The Netherlands

* Correspondence: j.tavora@utwente.nl

Table S1: Overview of in situ data.

Parameter	Unit	Source	Station	Sampling frequency	Period of data availability	SPM range
SPM	g.m^{-3}	RWS	*Hansweert Geul* *Hansweert 28* *Hoedekenskerke 4* *Pas van Terneuzen 10* *Schaar van Ouden Doel* *Terneuzen 20* *Vlissingen SSVH* *Zuidergat 49*	Bi-weekly to Monthly	$1984 - 2018$ $1984 - 1990$ $1988 - 2016$ $1984 - 1990$ $1984 - 2018$ $1984 - 2018$ $1984 - 2018$ $1984 - 1990$	$0.3 - 150.0$ $0.0 - 254.0$ $3.0 - 383.0$ $0.0 - 187.0$ $2.6 - 620.0$ $4.0 - 340.0$ $0.0 - 378.0$ $2.0 - 186.0$
SPM	g.m^{-3}	NIOZ	#1, 2, 3, 4, 13, 14, 16, 17	Bi-weekly	$1995 - 2004$	$4.1 - 509.2$
River discharge	m^3.s^{-1}	RWS	*Schaar van Ouden Doel*	Daily	$1984 - 2020$	
Wind speed/ direction	m.s^{-1}	KNMI	*Vlissingen – 310*	Hourly	$1984 - 2020$	
Water level	m	RWS	*Hansweert geul*	10min	$1984 - 2020$	

Table S2: Coefficients A and C of SPM algorithm. Original narrow-band and band-weighted coefficients (*A* and *C*; Equation 1 in main text) in the used SPM algorithm for each satellite sensor. Acronyms for satellite sensors are: TM (Thematic Mapper), ETM+ (Enhanced Thematic Mapper), and OLI (Operational Land Imager)

Satellite (sensor)	Central Band	Narrow-band		Band-weighted	
	[nm]	*A* [g.m^{-3}]	*C* [unitless]	*A* [g.m^{-3}]	*C* [unitless]
Landsat–5 (TM)	660	327.840	0.1708	331.589	0.1713
	839	2518.700	0.2105	2250.000	0.2093
Landsat–7 (ETM+)	661	333.728	0.1712	328.266	0.1710
	835	2379.770	0.2103	2270.300	0.2092
Landsat–8 (OLI)	655	289.290	0.1686	304.3023	0.1682
	865	2971.93	0.2115	2974.400	0.2115

Table S3: Match-up information data. In situ data is provided by RWS and by NIOZ. Refer to main text for full SPM data description. L5 is Landsat–5, L7 is Landsat–7, and L8 is Landsat–8.

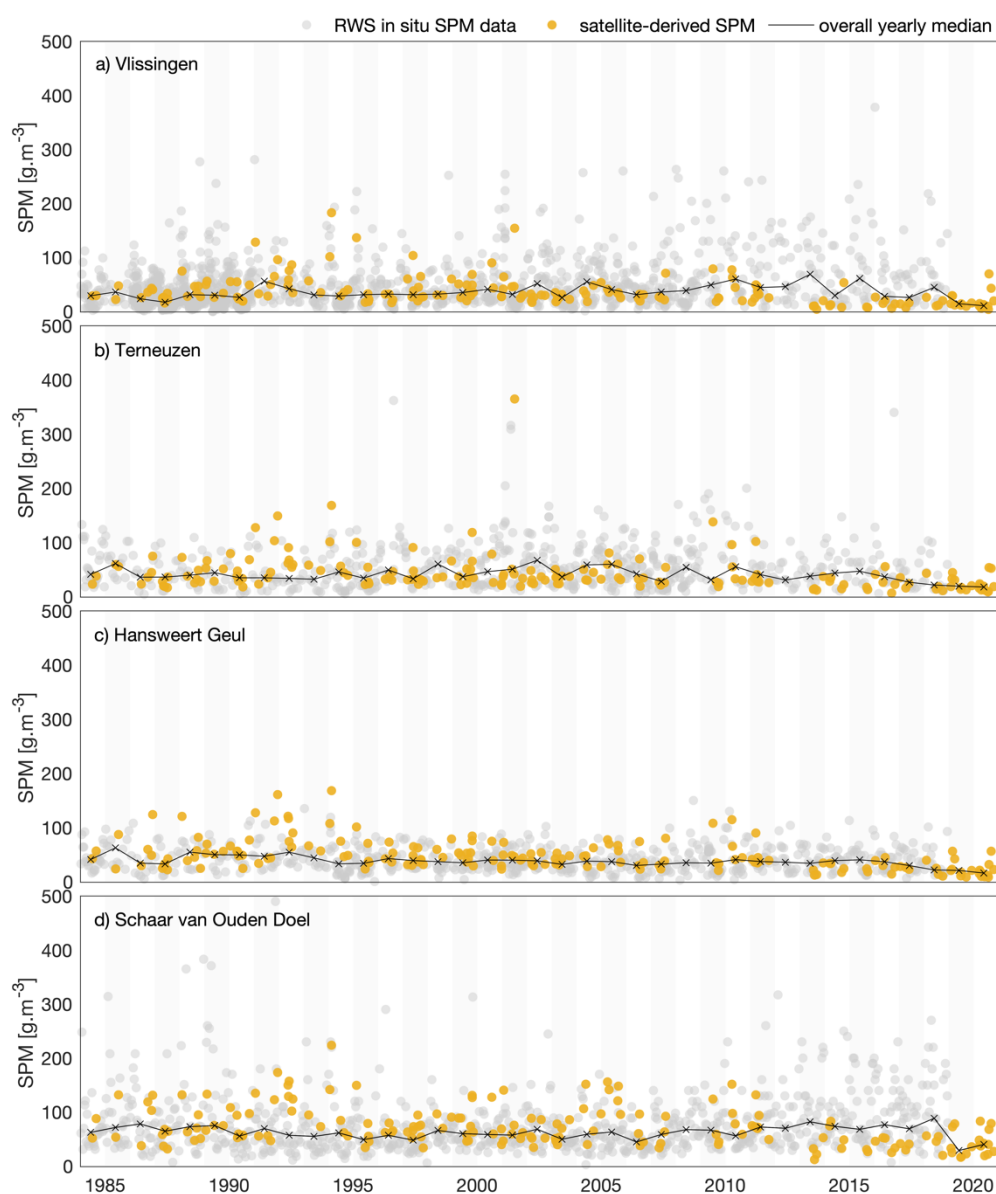| Date [yyyy.mm.dd] | Sampling time [UTC HH:mm:ss] | | Satellite | stations | SPM in-situ [g.m^{-3}] |
	satellite overpass	in situ			
1984.08.20	10:09:57	10:40:00	L5	RWS Hansweert Geul	42
		10:12:00	L5	RWS Hansweert 28	19
		09:10:00	L5	RWS Pas van Terneuzen 10	11
		11:09:00	L5	RWS Zuidergat 49	23
1986.09.20	09:54:14	10:00:00	L5	RWS Vlissingen SSVH	8
1987.04.23	10:03:13	11:00:00	L5	RWS Vlissingen SSVH	4
1988.04.25	10:10:12	09:10:00	L5	RWS Hansweert 28	9
		09:40:00	L5	RWS Pas van Terneuzen 10	15
		10:00:00	L5	RWS Pas van Terneuzen 10	18
		10:25:00	L5	RWS Vlissingen SSVH	22
1997.05.13	10:02:08	09:10:00	L5	RWS Terneuzen 20	45
		10:40:00	L5	RWS Terneuzen 20	16
1998.12.17	10:18:58	10:54:00	L5	NIOZ #16	75.1
		10:23:00	L5	NIOZ #17	97.48
1999.04.01	10:12:32	09:35:00	L5	RWS Schaar van Ouden Doel	50
1999.05.03	10:12:31	10:16:00	L5	RWS Schaar van Ouden Doel	43
2001.01.23	10:19:55	10:54:00	L5	NIOZ #17	95.75
2005.09.08	10:21:58	09:52:00	L5	RWS Schaar van Ouden Doel	99
1999.10.18	10:26:46	11:04:00	L7	RWS Hoedekenskerke 4	28
1999.11.03	10:26:43	10:31:00	L7	NIOZ #2	23.61
		10:50:00	L7	NIOZ #3	15.01
		10:00:00	L7	NIOZ #1	63.59
2003.03.19	10:22:33	09:35:00	L7	NIOZ #2	18.83
		09:50:00	L7	NIOZ #3	23.6
		10:40:00	L7	NIOZ #4	35.48
2014.09.08	10:40:10	11:23:00	L8	RWS Terneuzen 20	147
		10:06:00	L8	RWS Vlissingen SSVH	12

Figure S1. Interannual variability of SPM from in situ RWS datasets (grey scatter) and satellite-derived SPM (yellow scatter) relative to each region delimited in Figure 1 (main text). Overall yearly median is represented by black line.
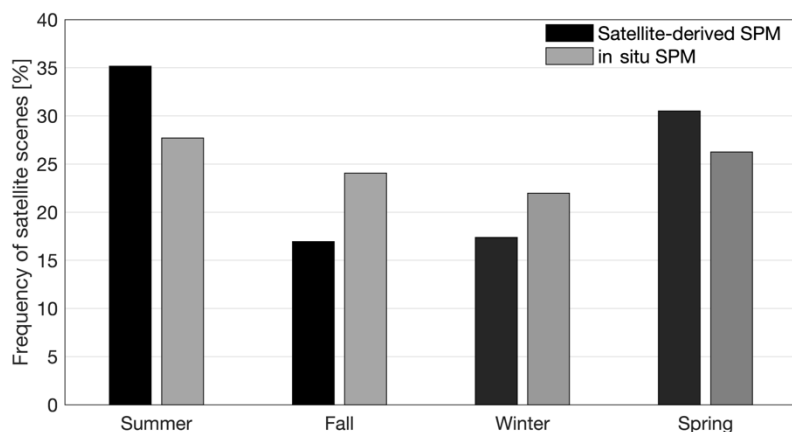
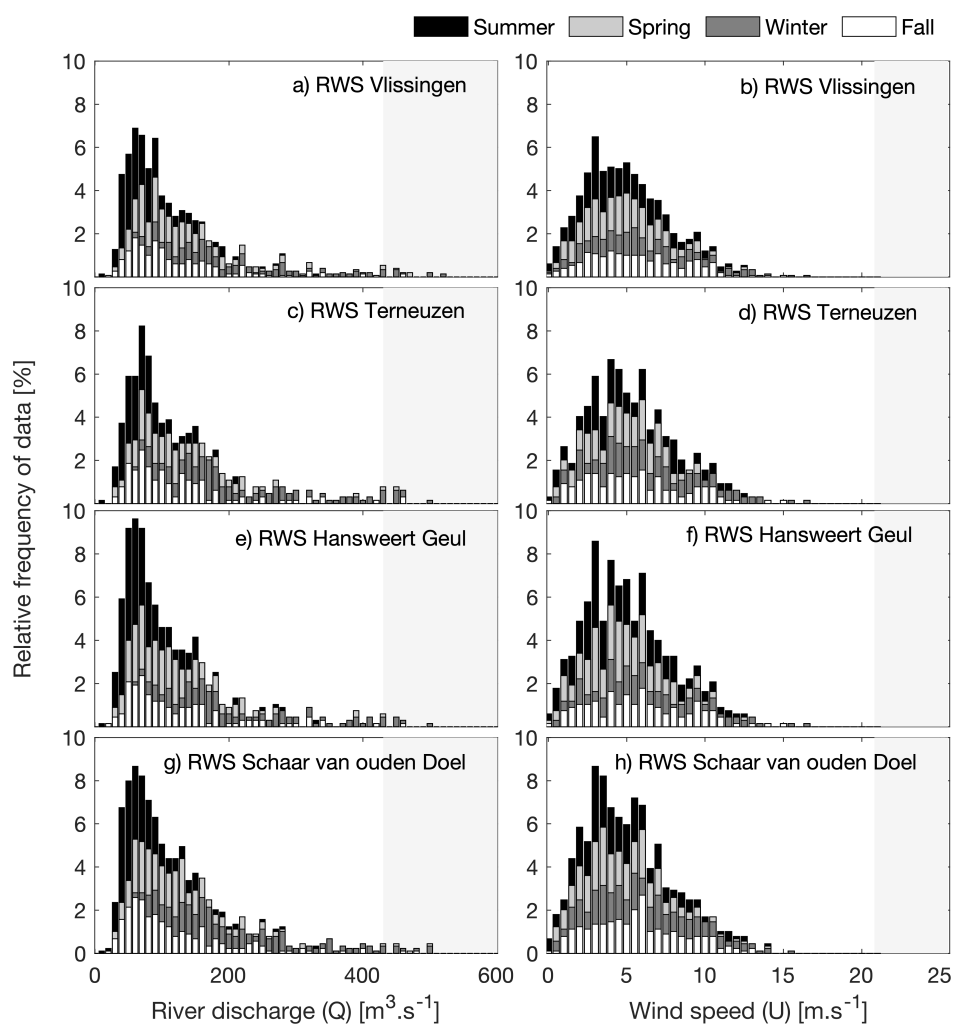Figure S2A. Distribution of total number of satellite scenes and in situ SPM per classes of boreal season

Figure S2B. Distribution of total number of in-situ SPM data (from in situ data RWS) per classes of boreal season (**a**) ,(**c**), (**e**), (**g**), daily river discharge and (**b**), (**d**), (**f**), (**h**), daily wind speed. Shared areas mark the threshold for extreme events.
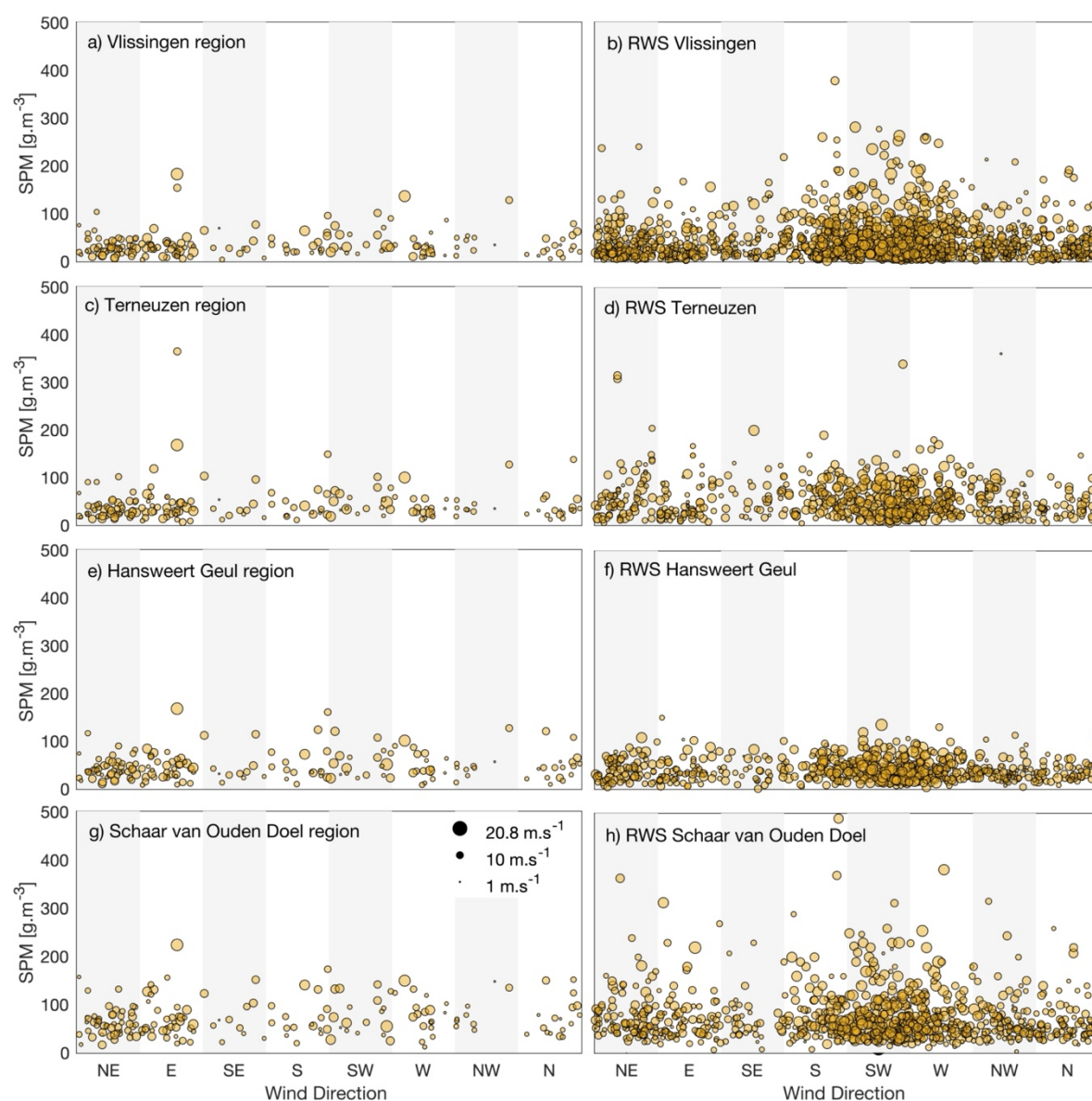
Figure S3 - *Relationship between wind direction and SPM. Panels (**a**), (**c**), (**e**), (**g**) represent the median satellite-derived SPM in the delimited region (refer to Figure 1 in main text). Panels (**b**), (**d**), (**f**), (**h**) represent the RWS long-term SPM in situ stations. Shaded areas represent each of the eight wind directions: northeast (NE centered at 45o), east (E; centered at 90o), southeast (SE; centered at 135o), south (S; centered at 180o), south-west (SW; centered at 225o), north-west (NW; centered at 315o), and north (N; centered at 0o or 360o). Scatter size is proportional to wind speed.*

Supplementary Material S1: Band-weighted uncertainties in the NIR bands

The range of wavelengths from available hyperspectral narrow-band coefficients (i.e., Table 1 and Table 4 in reference [1]) in Equation 1 (see main text), do not cover the spectral limits of SRFs (Spectral Response Functions) in the Near-InfraRed (NIR) of Landsat–5 (760-900nm), Landsat–7 (770-900nm) and Landsat–8 (829-900nm). Therefore, computed band-weighted coefficients (lacking the 885-900nm range) may introduce uncertainty to the SPM product, even though the band-weighted coefficients perform better than the narrow-band ones.

Reference [2] observed that uncertainties in coefficient C in Equation 1 have a negligible impact in SPM estimates while uncertainties in coefficient A translate as a linearly proportional misestimation in SPM due to the "settings" of the algorithm. Here, an uncertainty approximation for band-weighted coefficient A is computed based on a strong similarity between pure water absorption and the spectral curve of coefficient A (both normalized at 780nm) reported in reference [1]. With normalized pure water absorption equal to A, we computed the band-weighted A coefficient for each satellite sensor (1) in the full range of SRF (up until 900nm) and (2) limited by spectral range of the narrow band coefficients. Our extrapolated results in the NIR band show that band-weighted coefficient A is underestimated by 7.12% for Landsat–5, 6.26% for Landsat–7, and 0.03% for Landsat–8.

References:
1.   Nechad, B.; Ruddick, K.G.; Park, Y. Calibration and Validation of a Generic Multisensor Algorithm for Mapping of Total Suspended Matter in Turbid Waters. *Remote Sens. Environ.* **2010**, *114*, 854–866, doi:10.1016/j.rse.2009.11.022.

2.   Nechad, B.; Ruddick, K.G.; Neukermans, G. Calibration and Validation of a Generic Multisensor Algorithm for Mapping of Turbidity in Coastal Waters. *Remote Sens. Ocean. Sea Ice, Large Water Reg. 2009* **2009**, *7473*, 74730H, doi:10.1117/12.830700.